Bulletin of Geophysics and Oceanography Vol. XX, n. X, pp. XXX-XXX; Xxxxx 20xx
DOI 10.4430/bgo00508

# Earthquake engineering issues with bradyseism at Campi Flegrei: end 2024 - late 2025 update

P. Cito[1], R. Baraschino[2] and I. Iervolino[1,3]

[1] *Università degli Studi di Napoli Federico II, Napoli, Italy*
[2] *SPERI Società di Ingegneria S.p.A., Roma, Italy*
[3] *IUSS Scuola Universitaria Superiore, Pavia, Italy*

(Received: 7 July 2025; accepted: 13 October 2025; published online: 1 December 2025)

***ABSTRACT*** Between January and late September 2025, thousands of earthquakes were recorded at Campi Flegrei (southern Italy). These events are attributed to the ground uplift (currently a few centimetres per month) of the area due to volcanic activity, named bradyseism. Among the earthquakes of the sequence, which has lasted for some years so far, the largest estimated duration magnitude ($M_d$) reached 4.6. Complementing recent work by the authors, this study provides an updated analysis of the recent earthquakes from a structural engineering perspective. Focusing on earthquakes with $M_d \geq 2.5$ that occurred between March 2022 and September 2025, the study analyses the response spectra for the $M_d \geq 4.4$ events, maps the estimated shaking for the $M_d = 4.6$ earthquake of March 2025, and maps the envelopes of estimated shaking from all events considered. Finally, the structural response of equivalent single-degree-of-freedom (ESDoF) systems representative of code-conforming unreinforced masonry (URM) and reinforced concrete (RC) buildings, subjected to the whole sequence of $M_d \geq 2.5$ earthquakes, are discussed. Results show that the largest shaking of the sequence was recorded during the $M_d = 4.6$ event of March 2025, with peak ground accelerations greater than 0.7 g recorded at three stations within 1.6 km from the epicentre of the event. Nonlinear dynamic analysis of the ESDoF systems confirms that the impact of the sequence is negligible for the code-conforming RC structures, while the considered URM structure engages plastic excursions during the March $M_d = 4.6$ event, even in western Naples, and also during other events (mostly occurring in 2025) with $M_d$ between 3 and 4, and epicentral distance of about 1.5 km at most.

**Key words:** ground motion, shaking maps, masonry structures, reinforced concrete.

## 1. Introduction

Recent seismic activity in the Campi Flegrei volcanic area, near the city of Naples in southern Italy, has continued into 2025, which is attributed to ongoing bradyseism; i.e. the slow ground uplift and subsidence of the inner caldera of the volcano (Costa *et al*., 2021). The zone experiencing uplift, approximately a 5-kilometre radius area around Rione Terra and the downtown of Pozzuoli, is shown in Fig. 1a, although earthquakes are mostly occurring within 3 km from Rione Terra.

According to an earthquake catalogue specifically compiled for Campi Flegrei (Scotto di Uccio *et al*., 2024), approximately 9,000 events with duration magnitudes ($M_d$) ranging from –1.6 to 4.4 had been recorded between early 2014 and May 2024. In the 16 months spanning from May 2024 to September 2025, an additional 7,000 events were recorded by the Osservatorio

 

Vesuviano (OV) (https://terremoti.ov.ingv.it/gossip/flegrei/index.html, last accessed September 2025). According to the data, the epicentres of almost all the earthquakes are located within the municipality of Pozzuoli, where up to about 5,000 events per square kilometre were recorded, as shown in Fig. 1a.

The number of earthquakes also shows an increase in the last two years. Fig. 1b reports the cumulative number of recorded events since January 2014. By January 2023, the total had reached approximately 5,000. As of late 2025, more than 15,000 events had been recorded with $M_d$ ranging between -1.6 and 4.6. Fig. 1b also shows an increase in the number of earthquakes with $M_d \geq 2.5$ starting in 2022. From 16 March of the same year to 30 September 2025, approximately 160 of such events were recorded according to the OV, the most recent on 1 September. Among these, two events reached $M_d = 4.6$: the first on 13 March 2025 and the second on 30 June 2025.

Ground motion records for most of the $M_d \geq 2.5$ earthquakes recorded at Campi Flegrei are made available by the Rete Accelerometrica Nazionale (RAN) portal (https://ran.protezionecivile.it/IT, last accessed September 2025). The engineering analyses presented in this study were conducted using the records of all earthquakes with $M_d \geq 2.5$ and depth not exceeding 4 km, recorded from March 2022 to September 2025, available on the RAN portal. For six events that occurred between 13 May and 1 September 2025, recordings provided by the Istituto Nazionale di Geofisica e Vulcanologia (INGV) were used instead. Fig. 2 shows the position of the epicentres (dots) of the earthquakes with $M_d \geq 2.5$ considered (83 in number) and the seismic monitoring stations existing in the area, mostly belonging to the Italian Strong Motion Network (Felicetta *et al*., 2017). It is shown that most events, nine of which with $M_d \geq 4$, occurred inland Pozzuoli, near the Naples' border, with depths generally between 2 km and 3 km, while a few were located offshore. Station locations are indicated with colour-coded triangles indicating the soil class in accordance with the Eurocode 8 or EC8 classification (CEN, 2004). The EC8 class for each station is derived from the RAN portal, if available. Otherwise, the INGV classification is used. If neither RAN nor INGV provide a classification, the class by Forte *et al*. (2019) is represented in the figure.

More than 2,800 three-component (N-S, E-W, and vertical) accelerometric records (ASCII format) from the events with $M_d \geq 2.5$ in Fig. 2, together with response spectra at the stations, form a publicly available database (http://wpage.unina.it/iuniervo/CampiFlegrei_EQ_Records), which is continuously updated by the authors with $M_d \geq 2.5$ earthquakes, to support engineering analyses of the ongoing sequence. The database also includes maps of the (median) estimated

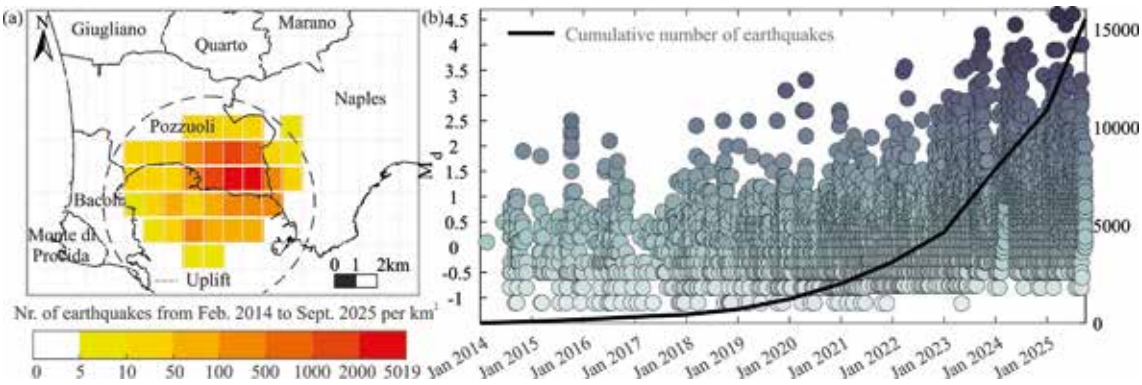


Fig. 1 - Number of earthquakes per square kilometre recorded between February 2014 and September 2025 (a) and uplift area with 5-kilometre radius (dashed circle); occurrence date, duration magnitude ($M_d$), and cumulative number of recorded earthquakes (b).

shaking in terms of both horizontal and vertical peak ground acceleration (*PGA*) and spectral pseudo-acceleration (*Sa*) (5% damped), at natural vibration periods $T$ = 0.3 s and $T$ = 1.0 s.

An investigation of ground shaking and engineering implications of seismicity at Campi Flegrei was already carried out by Cito *et al*. (2025), using available ground motion recordings from earthquakes with $M_d \geq 2.5$ recorded between August 2023 and December 2024. However, since this publication, new data for a relatively large number of events, with shaking of possible engineering interest, have become available. First, ground motion records for some events that occurred between 2023 and 2024 were added to the RAN portal only after Cito *et al*. (2025). Second, ground motion for about 40 earthquakes with $M_d \geq 2.5$ were recorded between January 2025 and late September 2025, including the two events, one in March and one in June, with the largest magnitude of the whole sequence, $M_d$ = 4.6.

The March $M_d$ = 4.6 earthquake is, in fact, a doublet event (Baltzopolous *et al*., 2025), which produced (unprocessed) *PGA* values greater than 0.7 g at three stations, namely the CSOB, COLB, and CFB3 (https://terremoti.ov.ingv.it/urbansm/flegrei/2025/44246, last accessed May 2025), with epicentral distance of 1.6 km at most (Fig. 3). The CSOB record, where the reliability of the waveforms is still debated by some, features 1.1 g horizontal *PGA* (unprocessed record), which may be the greatest *PGA* ever recorded in Italy to date (Suzuki and Iervolino, 2017). The greatest *PGA* for the $M_d$ = 4.6 earthquake of June is lower than 0.1 g. In fact, data in the compiled ground motion database show that, considering all the earthquakes with $M_d \geq 2.5$ following the $M_d$ = 4.6 of March 2025, the largest (horizontal) *PGA* is approximately 0.5 g, and it was recorded during the $M_d$ = 3.3 and $M_d$ = 4.0 events that occurred on 31 August and 1 September, respectively.

Fig. 2 also shows the greatest recorded *PGA* (black markers), *Sa*($T$ = 0.3 s) (green markers), and *Sa*($T$ = 1.0 s) (red markers) values for each station, which refer to both the horizontal (*H*) and vertical (*V*) components of motion, for the considered $M_d \geq 2.5$ events, indicated with square and dot markers, respectively. Using the same marker shape, the $M_d$ of the causative earthquake is represented for each intensity measure. The minimum and maximum epicentral distance ($R_{epi}$), at which the greatest shaking values, referring to the considered intensity measures, have been recorded, is also shown. At almost all stations, the strongest shaking was determined by one of the four earthquakes with $M_d \geq 4.4$, even when the station was closer to the epicentre of an event with $3.0 \leq M_d < 4.4$. Only a few stations recorded the largest ground motion (in terms of one of the considered spectral pseudo-accelerations) during an earthquake with $M_d < 4.4$. For instance, at the easternmost station in Pozzuoli, near the Naples' border, the highest horizontal *PGA*, approximately 0.5 g, was recorded during the $M_d$ = 3.9 earthquake that occurred on the evening of 16 February 2025. Metadata about the $M_d \geq 2.5$ events represented in Fig. 2, are provided in Appendix A. For each event, they include the number of recorded three-component records, minimum and maximum $R_{epi}$ at which they were recorded, and the largest recorded horizontal and vertical *PGA*s.

In the Fuorigrotta district of Naples, which borders with Campi Flegrei, the highest horizontal *PGA* was determined by the $M_d$ = 4.6 earthquake of March 2025 and reached about 0.2 g at stations with epicentral distances between 2 km and 6 km; i.e. about one fifth of the maximum value recorded near the epicentre in Pozzuoli. These data confirm a somewhat marked attenuation of the shaking towards Naples, a conclusion already reached in Cito *et al*. (2025). As expected, the attenuation is less pronounced for *Sa*($T$ = 0.3 s) and *Sa*($T$ = 1.0 s). This can be observed by comparing the maximum *PGA* and *Sa*($T$ = 1.0 s) intensities recorded in the $M_d$ = 4.4 event at epicentral distances shorter than 2 km and at the easternmost station in Naples (about 8 km from the epicentre).

The level of shaking recorded after December 2024, in both Pozzuoli and Naples, highlights the importance of assessing the structural engineering implications of the earthquakes recorded in 2025 at Campi Flegrei. This includes the analysis of the seismic structural actions, in terms of *Sa*(*T*), at four selected stations, considering the four largest magnitude earthquakes presented in Section 2. Maps of the largest estimated shaking in the area, provided in Section 3, are produced considering all the $M_d \geq 2.5$ events that have been recorded from 16 March 2022 to 30 September 2025 and for which ground motion data are available. Section 4 explores the structural response of nonlinear single degree-of-freedom systems equivalent to code-conforming residential masonry and reinforced concrete (RC) buildings in Pozzuoli, when subjected to the records from the whole $M_d \geq 2.5$ sequence, as recorded at four stations close to the epicentres of the largest magnitude events and in the Fuorigrotta district of Naples. Some final remarks close the study.

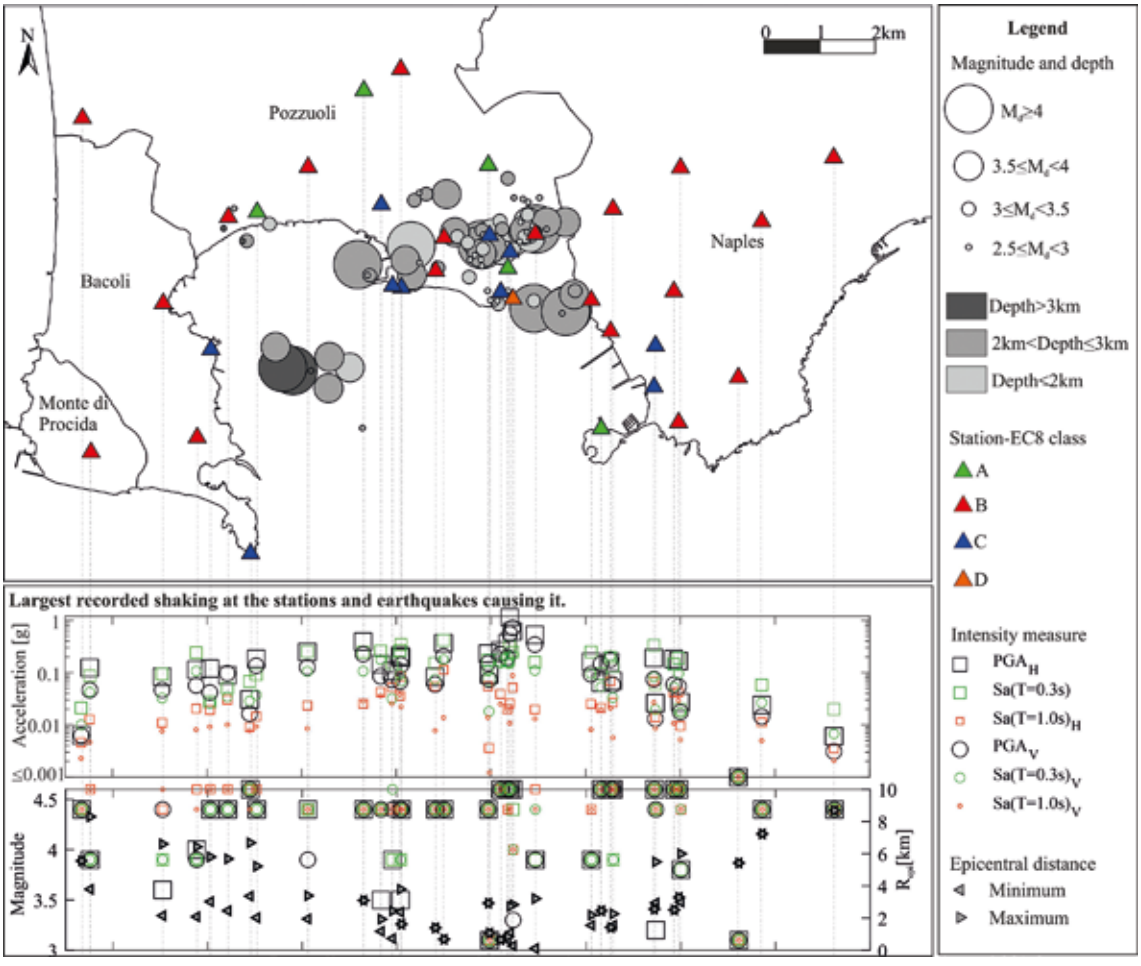


Fig. 2 - Epicentre, $M_d$, and depth of the $M_d \geq 2.5$ earthquakes recorded from March 2022 to September 2025, whose records are made available by RAN or INGV at the stations in the map. Below the map: the largest horizontal and vertical *PGA, Sa*(*T* = 0.3 s), and *Sa*(*T* = 1.0 s) recorded and the corresponding earthquakes in terms of $M_d$ and minimum and maximum $R_{epi}$.

## 2. Response spectra for the $M_d \geq 4.4$ earthquakes up to September 2025

This section presents the response spectra, in terms of *Sa*(*T*), of ground motion records from the four $M_d \geq 4.4$ earthquakes recorded at four selected seismic stations. They are the two events with $M_d = 4.4$ that occurred on 20 May 2024 and 13 May 2025, and the largest magnitude $M_d = 4.6$ events occurred on 13 March and 30 June 2025. According to a recently developed conversion relationship, $M_d = 4.4$ and $M_d = 4.6$ correspond to moment magnitude ($M_W$) of about 3.8 and 4.0, respectively, which means that the $M_W$ threshold of 4.4 (considered a reference value for the Campi Flegrei area) has barely or not been exceeded so far in the sequence (Iervolino *et al*., 2024).

Three of the selected stations are located in Pozzuoli and one is in Naples. The POZS (Pozzuoli Solfatara) and POZT (Pozzuoli Rione Terra) stations were selected because they recorded the strongest ground motion intensities during the 2024 $M_d = 4.4$ event, while the CSOB (Solfatara Bordo Cratere) was included as it recorded the largest *PGA* ever observed in Italy for the March 2025 $M_d = 4.6$ earthquake, if the recording can be considered reliable. The NAFG (Napoli Fuorigrotta) station was selected to analyse the shaking towards the city of Naples.

Fig. 3 shows the epicentres of the four earthquakes, the location of the selected stations, and the response spectra of the ground motion they recorded. The positions of the CFB3 and COLB stations are also indicated because, as mentioned, they recorded *PGA* values greater than 0.7 g

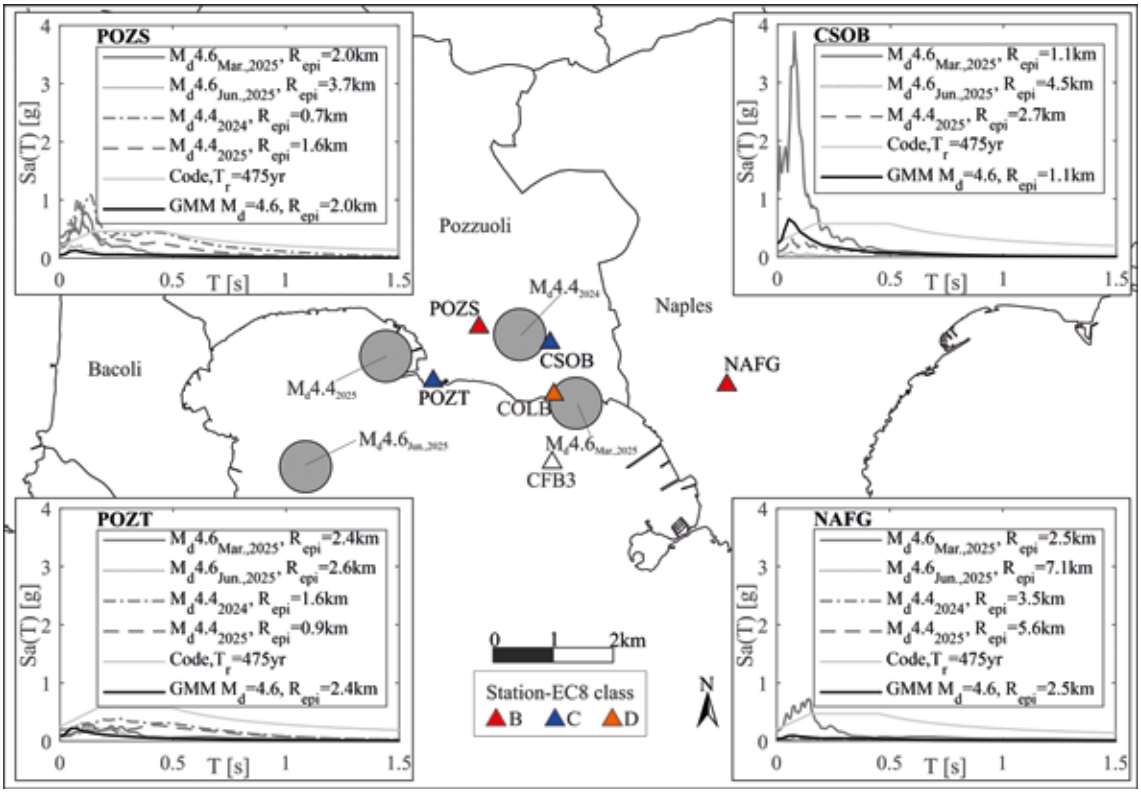


Fig. 3 - Magnitude and location of the $M_d \geq 4.4$ earthquakes recorded up to September 2025 and pseudo-acceleration response spectra at the CSOB, POZS, POZT, and NAFG stations. In each panel, the elastic design spectrum with 475-year return period and the median spectrum for the largest magnitude according to the selected GMM for Campi Flegrei are also shown.

during the March $M_d$ = 4.6 event; however, response spectra at these stations are not represented. Each spectrum provides, for each vibration period, the largest $Sa(T)$ among those for the two horizontal components of ground motion. As a reference, the (elastic) spectra provided by the Italian building code, the Norme Tecniche per le Costruzioni (NTC; CS.LL.PP., 2018), at the station sites, for the life-safety design of an ordinary construction, having exceedance return period of 475 years, according to long term probabilistic seismic hazard analysis [PSHA; Stucchi *et al*., (2011)], are represented. The median spectrum at each station for the largest magnitude event, according to a ground motion model (GMM) calibrated ad-hoc for the Campi Flegrei area, using data recorded between 2022 and 2024 (Iervolino *et al*., 2024), is also shown. Spectra account for the EC8 soil class of the stations in the figure.

At the CSOB station, the response spectrum of the March $M_d$ = 4.6 earthquake, which occurred 1.1 km from the station, has (if reliable) ordinates reaching about 4 g at vibration periods near 0.1 s. At increasing epicentral distances, between 2 km and 2.5 km, the spectral amplitude drops by more than 75%. Despite this rapid decrease, the ground motion recorded at the POZS and NAFG stations determined spectral ordinates as high as about 1 g and 0.7 g, respectively, thus exceeding, at high frequency of vibration, the elastic design spectrum with 475-year return period. Generally, these exceedances are expected in the case of close-by earthquakes, even if magnitude is relatively low (Iervolino *et al*., 2019). In fact, it should be noted that the $M_w$ of the event, $M_W \approx 4.0$, is even lower than the minimum magnitude used in the PSHA the design spectrum relies on (Stucchi *et al*., 2011). At the same time, such PSHA could not explicitly consider the peculiar features of earthquakes at Campi Flegrei, including shallowness and propagation, on which response spectra also depend.

The $M_d$ = 4.6 event of June was located offshore, with the considered stations at epicentral distances greater than 2.5 km. At the closest station, the POZT, the response spectrum reached approximately 0.25 g at 0.1 s and remained below the design spectrum for all vibration periods. In Naples, seismic actions can be deemed negligible, as the largest spectral ordinate at the NAFG remained below 0.02 g.

The two $M_d$ = 4.4 earthquakes caused seismic actions that exceeded the design spectrum, at some (relatively short or moderate) vibration periods, at the POZS station, the epicentral distance of which is not greater than 1.6 km for both events. For instance, the spectra exceed the design spectrum at periods lower than 0.15 s, and the spectrum for the $M_d$ = 4.4 of 2024 is comparable with the design counterpart for periods up to 0.6 s. At the CSOB station, the epicentral distance from the $M_d$ = 4.4 of 2025 is 2.7 km and spectral ordinates are below 0.15 g, while shaking from the $M_d$ = 4.4 of 2024 was not recorded.

Seismic structural actions at the NAFG station, located 3.5 to 5.6 km from the epicentres, can be deemed negligible for both $M_d$ = 4.4 events. This indicates that, among all (the considered) $M_d \geq 2.5$ events recorded in the Campi Flegrei area over the past three years and a half, only the March 2025 $M_d$ = 4.6 generated ground motion in Naples that may have a relevance from the structural engineering perspective.

## 3. Estimated shaking on a territorial scale

At unmonitored locations, shaking in terms of one ground motion intensity measure caused by an earthquake can be estimated using the ShakeMap approach (Wald *et al*., 1999). ShakeMap is currently based on the assumption that the logarithms of the intensity measure at the locations of interest follow a multivariate normal (MVN) distribution, conditional on the

earthquake's magnitude and location, soil site conditions, and on the recordings at monitoring stations (Worden *et al*., 2018). ShakeMap requires a GMM and a correlation model for GMM within-event residuals.

For earthquakes that occurred at Campi Flegrei, INGV provides ShakeMap in terms of *PGA*, *Sa*(*T* = 0.3 s), *Sa*(*T* = 1.0 s), peak ground velocity (PGV), and macroseismic intensity in terms of Mercalli-Cancani-Sieberg scale. The GMM considered is that of Tusa and Langer (2016), which was developed specifically for the Etna volcanic region. Therefore, using the GMM from Iervolino *et al*. (2024), the mean vector and the covariance matrix of the MVN distributions of the logarithms of *PGA*, *Sa*(*T* = 0.3 s), and *Sa*(*T* = 1.0 s) were computed at the sites corresponding to the nodes of a grid, with less than 100-metre spacing, discretising the inland area, for the March 2025 $M_d$ = 4.6 earthquake, which caused relatively significant seismic actions even in Naples (see previous section). In the calculations, the EC8-C soil class was assumed everywhere, as it is the one attributed to most sites in the area (Forte *et al*., 2019; Michelini *et al*., 2019). The spatial correlation of GMM within-event residuals was modelled according to Esposito and Iervolino (2012), while between-event residuals were assumed to be perfectly correlated (Giorgio and Iervolino, 2016). The MVN distribution is conditioned on shaking values recorded at stations with $R_{epi}$ up to 40 km, to avoid extrapolation of the GMM.

Fig. 4a shows the median values of the largest horizontal *PGA* at each site, which is the typical representation of ShakeMap. The values at the station sites are the recorded intensities (largest between the two horizontal components) constraining the calculations. The largest median *PGA* is estimated at the east of Pozzuoli downtown, due to the CSOB station record (see Section 1). At a distance of about 2 km from the epicentre, the *PGA* is already reduced by more than half with respect to the greatest estimated value. In most of the area, the estimated *PGA* is below 0.05 g.

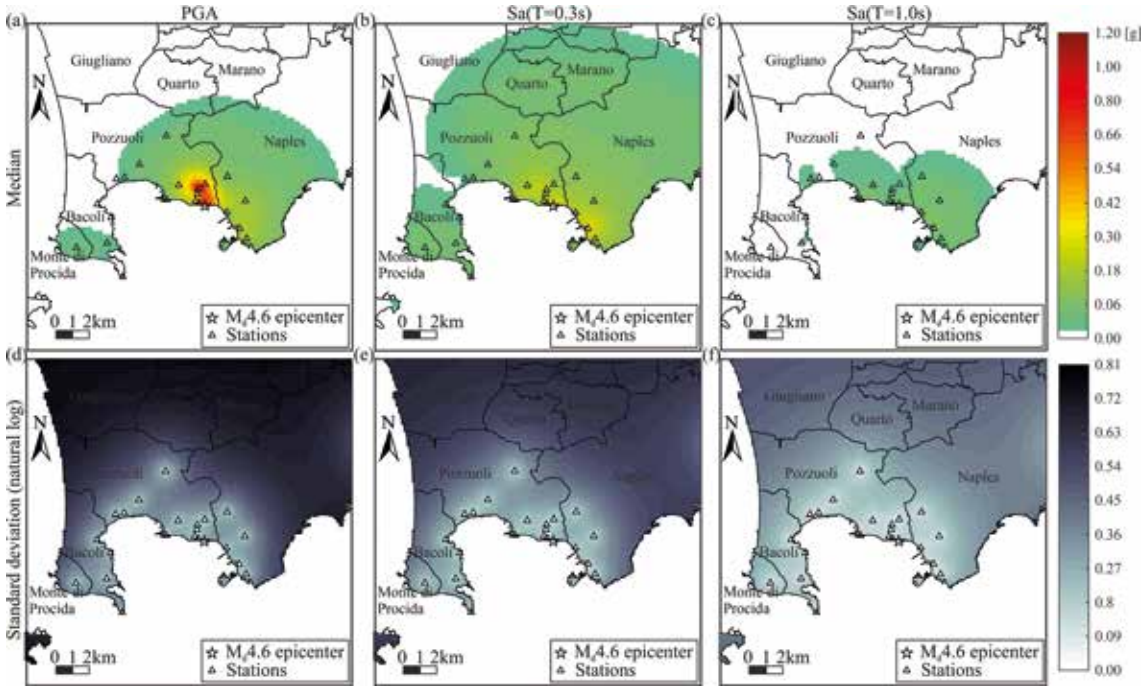


Fig. 4 - Maps of the median (panels a to c) and standard deviation (panels d to f) of the natural logarithm of the shaking, in terms of largest horizontal *PGA, Sa*(*T* = 0.3 s), and *Sa*(*T* = 1.0 s) for the $M_d$ = 4.6 earthquake which occurred on 13 March 2025.

As expected from recorded intensities, the shaking map, in terms of *Sa*(*T* = 0.3 s), shows a less pronounced attenuation with distance compared to *PGA,* as indicated by the greatest estimated values of approximately 0.3 g both near the epicentre and more than 3 km away from it, towards SW Naples (e.g. the Bagnoli district). In the case of *Sa*(*T* = 1.0 s), the estimated intensity is lower than 0.1 g near the epicentre and is generally below 0.01 g in most of the area.

To quantify the uncertainty affecting the shaking, the standard deviation (of the natural logarithm) of the intensity measure was also computed. It is represented in Fig. 4d for *PGA*, while Figs. 4e and 4f refer to *Sa*(*T* = 0.3 s) and *Sa*(*T* = 1.0 s). Standard deviation is zero at the station sites, whereas, away from them, it progressively increases tending to that of the GMM total residual (between-event plus within-event), as the conditioning effect of the stations tends to vanish far from them.

Similar considerations regarding the attenuation of the estimated shaking and the associated uncertainty apply to the vertical component of ground motion, as shown by the maps in Fig. 5. These maps were generated following the same procedure as for the horizontal shaking (Fig. 4), yet using vertical GMM for Campi Flegrei and conditioning the MVN distribution to the vertical rather than to the horizontal records. The vertical-to-horizontal ratio for the median estimated shaking of the $M_d$ = 4.6 event is 0.6 for *PGA*, 0.5 for *Sa*(*T* = 0.3 s), and 0.4 for *Sa*(*T* = 1.0 s), for sites within a 5-kilometre epicentral distance. These values are in accordance with Ramadan *et al*. (2021) for $M_W$ = 4.0.

In Cito *et al*. (2025), the envelopes of the median shaking maps (Allen *et al*., 2009; Iervolino *et al*., 2021), for all earthquakes with $M_d \geq 2.5$ that occurred between 18 August 2023 and 6 December 2024, were presented. For each site, the envelopes provide the largest median intensity among all events considered. Since the maps in Figs. 4 and 5 have shown that the horizontal and

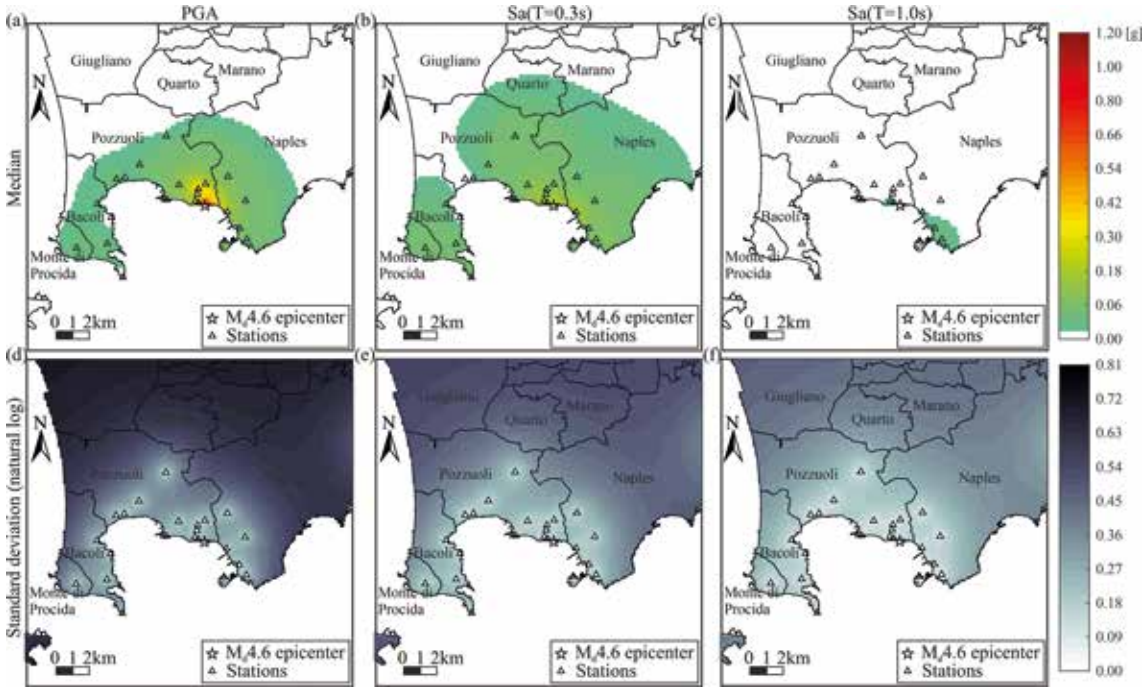


Fig. 5 - Maps of the median (panels a to c) and standard deviation (panels d to f) of the natural logarithm of the shaking, in terms of vertical PGA, *Sa*(*T* = 0.3 s), and *Sa*(*T* = 1.0 s) for the $M_d$ = 4.6 earthquake which occurred on 13 March 2025.

vertical estimated shaking caused by the March 2025 $M_d$ = 4.6 earthquake exceeds 1 g and 0.5 g, respectively, near the epicentre, and considering that some events in 2025 produced larger shaking than those recorded in 2024 at the same stations and for the same magnitudes, it is useful to update such envelopes with all the events between March 2022 and September 2025. The updated envelopes are presented in Fig. 6 for the horizontal and vertical components of ground motion. The maps also show the epicentres and the related recording stations (the $M_d$ = 2.5 event of December 2024 was excluded due to the alleged unreliability of recordings at one station; as a result, the envelopes, along with the structural analyses presented in the following, account for 82 earthquakes in lieu of 83).

A comparison between the envelope maps and those for the event in Figs. 4 and 5 reveals substantial differences in Pozzuoli, where the epicentres are located. Smaller or negligible differences are observed in the rest of the area, indicating dominance of the largest magnitude earthquake event that occurred on 13 March 2025 in terms of maximum (estimated) intensity. For instance, considering the horizontal *PGA* (Fig. 6a), the area in Pozzuoli, where the median shaking exceeds 0.3 g, expands considerably towards the municipality of Bacoli in the envelope compared to what observed for $M_d$ = 4.6 (Fig. 4a). Still in Pozzuoli, the median shaking from the earthquakes with magnitude lower than 4.6, including some with $M_d$ < 4, is greater than the $M_d$ = 4.6 counterpart over a large area even for $Sa(T = 0.3\ s)$ and $Sa(T = 1.0\ s)$. In Naples, by contrast, the envelope maps do not significantly differ from those of the March 2025 $M_d$ = 4.6 earthquake. However, the contributions of the $M_d \geq 2.5$ events to the envelope can be examined via event-specific shaking maps (together with the data required to reproduce them available at http://wpage.unina.it/iuniervo/CampiFlegrei_EQ_Records).

## 4. Structural response of code-conforming buildings

Nonlinear dynamic analyses discussed in Cito *et al*. (2025) showed that, among the $M_d \geq 2.5$ earthquakes recorded between August 2023 and December 2024, only the largest one had a non-negligible structural impact. However, the ground motion analysis of the 2025 earthquakes, presented in the previous sections, suggests the need to update those analyses. This is not only because the seismic actions recorded in 2025 are stronger than those in 2024, even for the same magnitude and epicentral distance, but also because some earthquakes recorded in 2025 have produced significant shaking, at short vibration periods, even at locations not necessarily within 1 km from the epicentre, something that does not emerge when considering only the events that occurred up to the end of 2024.

Although the existing building stock in Campi Flegrei is mainly composed of residential buildings built with obsolete or absent seismic provisions (Iervolino *et al*., 2024), this section evaluates the structural impact of the recorded ground motions on buildings designed according to the seismic code currently enforced. Two cases are analysed: an unreinforced masonry (URM) structure and a RC moment-resisting frame. These typologies together represent nearly 90% of the stock in Pozzuoli.

The URM structure is a two-story building, regular in plan and elevation, while the RC structure is a three-story bare frame. The structural models were developed within the RINTC project (RINTC-Workgroup, 2018). Design was carried out assuming that the structures were located in Naples on C-type site conditions according to EC8. Each structure was modelled as an equivalent single-degree-of-freedom (ESDoF) system (Suzuki and Iervolino, 2021). The equivalent vibration period is $T$ = 0.07 s for the URM ESDoF system and $T$ = 0.93 s for the RC one. The backbone curves

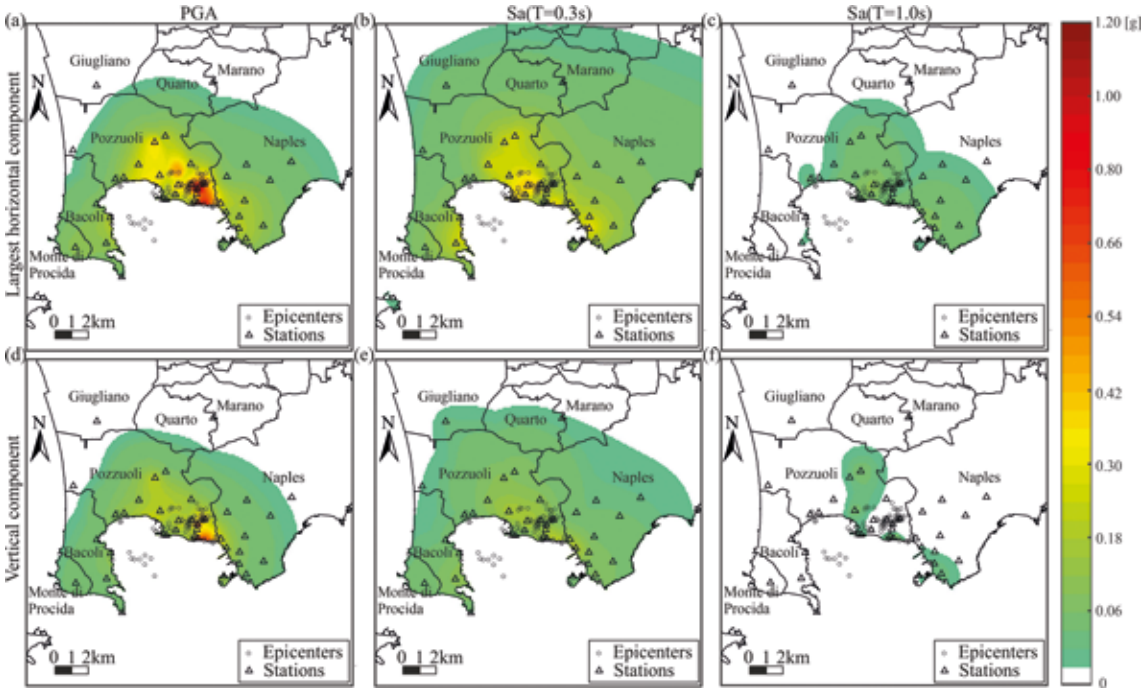


Fig. 6 - Maps of largest median shaking from the $M_d \geq 2.5$ events recorded from March 2022 to September 2025, in terms of *PGA, Sa*($T$ = 0.3 s), and *Sa*($T$ = 1.0 s). Considered events are those whose records are made available by RAN or INGV. Panels a to c and panels d to f refer to the largest horizontal and vertical ground motion components, respectively.

and their parameters, for the two ESDoF systems, are shown in Cito *et al*. (2025). It results that the yielding spectral acceleration for the URM and RC structures are $Sa_{y,URM}(T = 0.07\ s) = 0.52$ g and $Sa_{y,RC}(T = 0.93\ s) = 0.31$ g, respectively. For both systems, the hysteretic behaviour is pinched peak-oriented (Lowes *et al*., 2004) with no degradation for both systems and equivalent viscous damping factor of 5%.

The two structural models were virtually placed at the sites of stations POZS, POZT, CSOB, and NAFG, and analysed using the records at the considered sites as input. More specifically, each ESDoF system was subjected to four record sequences, each constructed by appending all signals from the 82 earthquakes with $M_d \geq 2.5$ (those considered for the envelope of the shaking maps) recorded at the selected stations. The sequence at a site can differ from the analyses for the URM and RC systems because, for each earthquake, the horizontal component with the largest spectral ordinate at the period of the considered ESDoF system was selected. Moreover, the time between two earthquake-specific records, during which the ESDoF system is in free vibrations, was set equal to ten times the ESDoF period.

The results of the analyses, in terms of hysteretic response, are shown in Fig. 7. The RC system never exhibits plastic behaviour engagement, with the residual displacement (cyan marker) being zero at all the four sites of the stations considered. This indicates that seismic activity recorded so far at Campi Flegrei has effects that can be deemed negligible for this building typology, even in Pozzuoli, within 1 km from the epicentres of the $M_d \geq 4.4$ events. The same conclusion cannot be drawn for the URM system, which exhibits engagement of nonlinear behaviour at three out of the four stations, including the CSOB, POZS, and NAFG in western Naples. The largest structural impact is observed at the CSOB station, as expected. The ground motion records at this station produce a maximum transient displacement (blue marker) approaching 0.3 cm, more than five

times the yield displacement, while the residual displacement is approximately 0.2 cm.

Fig. 7 shows that the structural impact of the $M_d \geq 2.5$ earthquakes is less severe at the POZS station than at the CSOB station, and it further decreases from the CSOB to the NAFG. To deepen this issue, the earthquakes that induce plastic excursion at each station were first identified. They are those with the record at the station, which has been used in the dynamic analysis, having $Sa(T = 0.07\ \text{s}) > Sa_{y,URM}(T = 0.07\ \text{s})$. The date, duration magnitude, epicentral distance, and depth of these events are listed in Table 1, along with the $Sa(T = 0.07\ \text{s})$ value of the selected horizontal component of ground motion.

It is observed that the five earthquakes, causing the URM ESDoF system to exhibit inelastic behaviour at the CSOB station, occurred between January and July 2025, all with epicentral distances smaller than 1.5 km. Depths are between 1.6 km and 2.7 km and hypocentral distances are shorter than 3 km. In addition to the March event, these events include the event of 18

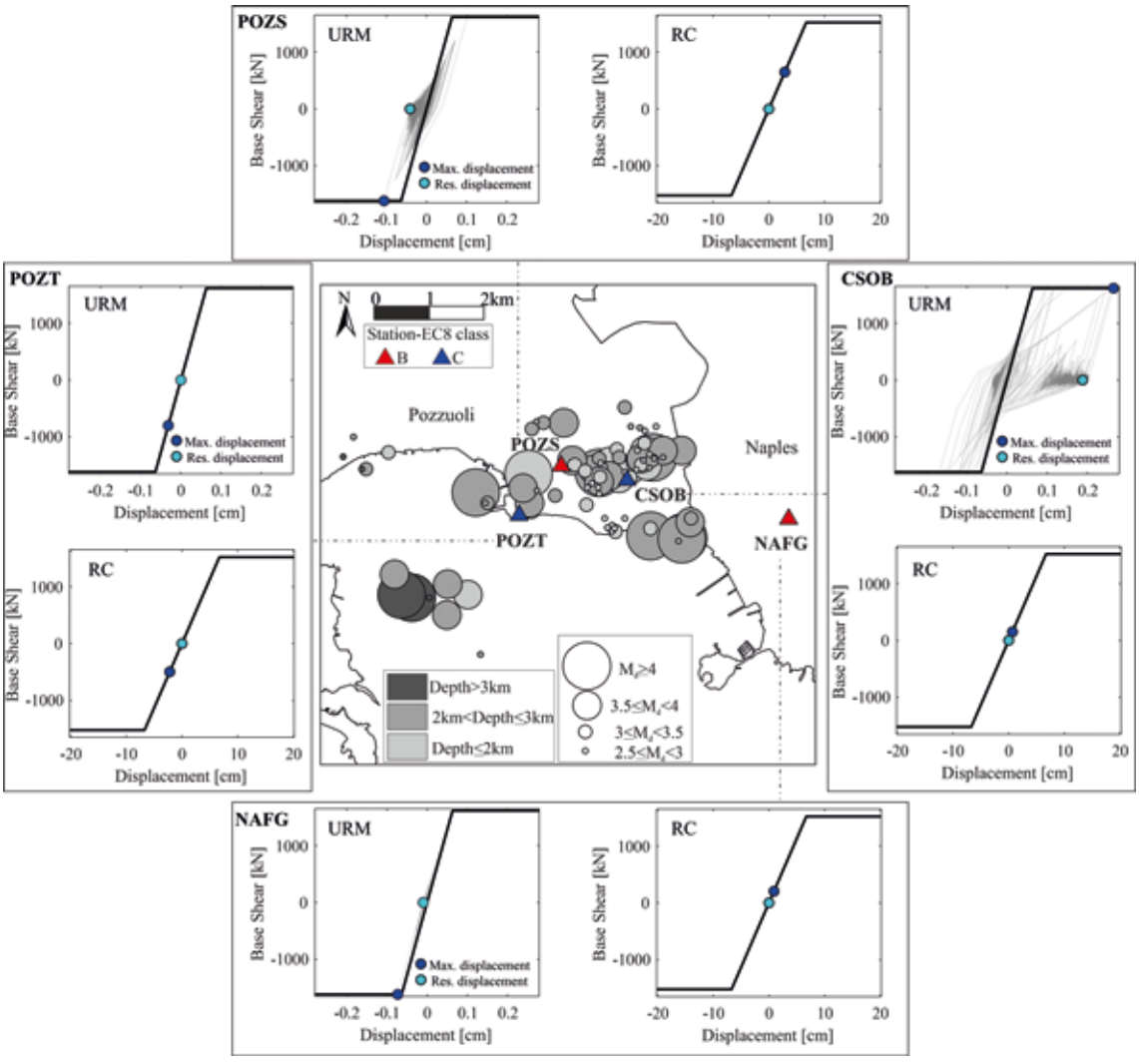


Fig. 7 - Results of nonlinear dynamic analysis for the URM and RC ESDoF systems subjected to records from earthquakes with $M_d \geq 2.5$ recorded at the CSOB (right), POZS (top), POZT (left) and NAFG (bottom) stations. Station sites and earthquake magnitude, depth, and epicentres are shown in the central panel.

July and three events with $M_d$ < 4.0, namely the $M_d$ = 3.9, mentioned in Section 1 (i.e. the one causing a *PGA* of 0.5 g near its epicentre; see Fig. 2), the $M_d$ = 3.2, and the $M_d$ = 3.0 ones that occurred in June and January, respectively. At the POZS station, plastic excursion occurs due to seven earthquakes with magnitude between 3.1 and 4.4, all with $R_{epi}$ from 0.2 km to 1.6 km. Earthquake depths are between 2.2 km and 2.9 km and hypocentral distance varies from 2.3 km to 3.0 km. Five out of seven earthquakes occurred in 2025, while the others are the largest magnitude event of May 2024 and the $M_d$ = 3.5 event that occurred in March 2022. At the NAFG station, nonlinear behaviour is seen only for the March 2025 $M_d$ = 4.6 event.

For each event causing plastic excursion of the ESDoF system, the energy demand in terms of number of equivalent cycles ($n_{eq}$) was, then, calculated. It represents the number of cycles at the maximum plastic displacement that the structure can undergo to dissipate the total hysteretic energy. It was computed following the approach proposed by Manfredi (2001), leading to the following equation for the considered URM system:

$$n_{eq} = 1 + 0.18 \cdot \left( \frac{Sa(T = 0.07\ \mathrm{s})}{Sa_{y,URM}(T = 0.07\ s)} - 1 \right)^{3/5} \cdot \frac{I_a \cdot 2 \cdot g/\pi}{PGA \cdot PGV} \cdot \left( \frac{Sa(T = 0.07\ \mathrm{s})}{0.5} \right)^{-0.5} \quad (1)$$

where *PGV* is the peak ground velocity of the record the structure is subjected to, and $I_a$ is the Arias intensity. Table 1 provides the values of $n_{eq}$ at each station and also summarises the data for calculation. It is shown that, at the CSOB station, $n_{eq}$ is greater than 15 for the $M_d$ = 4.6 event, at least three times the corresponding value for the other events. At the POZS station, the hysteretic dissipated energy due to the $M_d$ = 4.4 event of 2024 is comparable to that for the $M_d$ = 3.9 event of March 2025. When the URM system is located at the NAFG station, the plastic excursion caused by the $M_d$ = 4.6 event is limited compared to when the structure is at an epicentral distance of about 1 km, with $n_{eq}$ being roughly one tenth of the value at the CSOB.

It is worth noting that, at two out of the three stations, nonlinear behaviour is caused by the March 2025 $M_d$ = 4.6 earthquake (at least). This is not the case at the POZS station, where *Sa*(*T* = 0.07 s) caused by the same event is equal to 0.48 g, despite the epicentral distance (2 km; see Fig. 3) being slightly shorter than that of the NAFG station. At the POZT station, all the records

Table 1 - Earthquakes inducing plastic excursion to the URM ESDoF system at the CSOB, POZS, and NAFG stations.

| Station | Date | $M_d$ | $R_{epi}$ [km] | Depth [km] | *Sa*(*T* = 0.07 s) [g] | *PGA* [g] | *PGV* [m/s] | $I_a \cdot 2 \cdot g/\pi$ [m²/s³] | $n_{eq}$ |
|---|---|---|---|---|---|---|---|---|---|
| CSOB | 17/01/2025 | 3 | 0.98 | 1.72 | 0.62 | 0.16 | 0.02 | 0.29 | 2.66 |
| | 16/02/2025 | 3.9 | 0.44 | 1.59 | 0.97 | 0.33 | 0.05 | 1.81 | 5.83 |
| | 13/03/2025 | 4.6 | 1.09 | 2.50 | 3.31 | 1.14 | 0.11 | 13.00 | 15.29 |
| | 05/06/2025 | 3.2 | 0.58 | 2.67 | 0.67 | 0.18 | 0.03 | 0.32 | 2.43 |
| | 18/07/2025 | 4 | 1.44 | 2.53 | 0.58 | 0.21 | 0.03 | 0.45 | 1.80 |
| POZS | 20/05/2024 | 4.4 | 0.68 | 2.57 | 0.83 | 0.27 | 0.07 | 1.76 | 4.13 |
| | 13/05/2025 | 4.4 | 1.61 | 2.61 | 0.64 | 0.18 | 0.06 | 0.88 | 2.71 |
| | 15/03/2025 | 3.9 | 0.22 | 2.86 | 0.65 | 0.15 | 0.03 | 0.46 | 3.39 |
| | 16/03/2022 | 3.5 | 0.88 | 2.54 | 0.53 | 0.13 | 0.02 | 0.26 | 1.26 |
| | 13/05/2025 | 3.3 | 0.84 | 2.57 | 0.68 | 0.15 | 0.02 | 0.38 | 3.96 |
| | 14/05/2025 | 3.1 | 1.55 | 2.49 | 0.56 | 0.19 | 0.03 | 0.29 | 1.48 |
| | 06/06/2025 | 3.2 | 0.43 | 2.23 | 0.71 | 0.20 | 0.03 | 0.25 | 2.31 |
| NAFG | 13/03/2025 | 4.6 | 2.51 | 2.50 | 0.59 | 0.18 | 0.05 | 0.66 | 2.13 |

considered in the analyses have $Sa(T = 0.07\ s) < Sa_{y,URM}(T = 0.07\ s)$ and, therefore, the URM system remains elastic in all events. Finally, Table 1 does not contemplate the RC ESDoF system, since $Sa(T = 0.93\ s)$ is lower than $Sa_{y,RC}(T = 0.93\ s)$ for all the records considered in the dynamic analyses. This confirms, as already mentioned, that the considered RC system remains elastic at all station sites and under all considered earthquakes.

## 5. Final remarks

Since 2014, approximately 15,000 earthquakes, with $M_d$ ranging from -1.6 to 4.6, have been recorded in the Campi Flegrei area, which is currently undergoing slow uplift due to volcano dynamics known as bradyseism. Two among these events are attributed $M_d = 4.6$. They were recorded in March and June 2025. Since the beginning of 2025, about 40 earthquakes with $M_d \geq 2.5$ have been recorded and can be used for structural engineering analyses thanks to the availability of ground motion records. The present study is an update to previous work on the earthquake engineering aspects of the seismic activity accompanying bradyseism at Campi Flegrei, considering the earthquakes with $M_d \geq 2.5$ recorded from 16 March 2022 to 30 September 2025. The main findings are summarised below.

- So far, largest bradyseism-induced seismic actions were recorded during the $M_d = 4.6$ of March 2025, close to its epicentre. At three stations in Pozzuoli, with epicentral distance of 1.6 km at most, the recorded *PGA* is greater than 0.7 g and spectral ordinates reached (if reliable) about 4 g at vibration periods near 0.1 s. The shaking from the $M_d = 4.6$ event of March is the strongest of the sequence also in western Naples, at about 2.5 km from the epicentre. The $M_d = 4.6$ of June determined values of *PGA* lower than 0.1 g, and spectral ordinates at Pozzuoli, at a 2.5-kilometre epicentral distance, do not exceed 0.25 g.
- The comparison between the maps of the estimated shaking for the March 2025 $M_d = 4.6$ event and those of the largest estimated shaking for all the $M_d \geq 2.5$ earthquakes shows that the strongest magnitude event of the sequence dominates, in terms of estimated shaking, in western Naples. In Pozzuoli, the largest estimated shaking is also attributed to other events, including some with $M_d < 4.0$.
- The code-conforming URM structure examined engages inelastic behaviour due to 10 earthquakes with $3.0 \leq M_d \leq 4.6$ recorded from January 2025 to July 2025, the $M_d = 4.4$ of May 2024, and the $M_d = 3.5$ of March 2022. Plastic excursion is observed at an epicentral distance of about 1.5 km at most for almost all events, and at 2.5 km, in western Naples, for the $M_d = 4.6$ of March 2025. The number of equivalent cycles shows that, for the latter event, the hysteretic energy dissipated by the URM structure increases by one order of magnitude as its epicentral distance decreases from 2.5 km to 1.1 km. The structural impact on the considered code-conforming RC structure can be deemed negligible for each of the considered $M_d \geq 2.5$ events and even in proximity of their epicentres.

**Acknowledgments.** The presented study was developed within the framework of the Rete dei Laboratori Universitari di Ingegneria Sismica (ReLUIS) within the 2024−2026 ReLUIS-DPC research program. Ground motion records, metadata, and estimated shaking maps for all the considered events are available at http://wpage.unina.it/iuniervo/CampiFlegrei_EQ_Records. The authors would also like to thank Stefano Parolai and one anonymous reviewer for their comments that improved the quality and readability of this paper.

REFERENCES

Allen T.I., Wald D.J., Earle P.S., Marano K.D., Hotovec A.J., Lin K. and Hearne M.G.; 2009: *An atlas of ShakeMaps and population exposure catalog for earthquake loss modeling.* Bull. Earthq. Eng., 7, 701–718, doi: 10.1007/s10518-009-9120-y.

Baltzopolous G., Baraschino R., Cito P., Colombelli S., Delouis B., De Landro G., Elia L., Festa G., Iaccarino A.G., Herrmann M., Iervolino I., Longobardi V., Marzocchi W., Nazeri S., Palo M., Russo G., Scala A., Scotto di Uccio F., Sollai A., Strumia C. and Zollo A.; 2025: *Doublet earthquake at Campi Flegrei 13 March 2025. Version 2.* Zenodo, doi: 10.5281/zenodo.15046784.

CEN; 2004: *Eurocode 8: design provisions for earthquake resistance of structures, Part 1.1: general rules, seismic actions and rules for buildings.* PrEN 1998-1, European Committee for Standardisation, Brussels, Belgium.

Cito P., Baraschino R. and Iervolino I.; 2025: *Ground motion, estimated shaking, and structural response at Campi Flegrei during bradyseism.* Earthq. Eng. Struct. Dyn., 54, 1313–1323, doi: 10.1002/eqe.4303.

Costa A., Di Vito M.A., Ricciardi G.P., Smith V.C. and Talamo P.; 2021: *The long and intertwined record of humans and the Campi Flegrei volcano (Italy).* Bull. Volcanol., 84, 5, doi: 10.1007/s00445-021-01503-x.

CS.LL.PP.; 2018: *Aggiornamento delle Norme tecniche per le costruzioni (in Italian).* Gazzetta Ufficiale della Repubblica Italiana, 42, Roma, Italy.

Esposito S. and Iervolino I.; 2012: *Spatial correlation of spectral acceleration in European data.* Bull. Seismol. Soc. Am., 102, 2781–2788, doi: 10.1785/0120120068.

Felicetta C., D'Amico M., Lanzano G., Puglia R., Russo E. and Luzi L.; 2017: *Site characterization of Italian accelerometric stations.* Bull. Earthq. Eng., 15, 2329–2348, doi: 10.1007/s10518-016-9942-3.

Forte G., Chioccarelli E., De Falco M., Cito P., Santo A. and Iervolino I.; 2019: *Seismic soil classification of Italy based on surface geology and shear-wave velocity measurements.* Soil Dyn. Earthq. Eng., 122, 79–93, doi: 10.1016/j.soildyn.2019.04.002.

Giorgio M. and Iervolino I.; 2016: *On multisite probabilistic seismic hazard analysis.* Bull. Seismol. Soc. Am., 106, 1223–1234, doi: 10.1785/0120150369.

Iervolino I., Giorgio M. and Cito P.; 2019: *Which earthquakes are expected to exceed the design spectra?* Earthq. Spectra, 35, 1465–1483, doi: 10.1193/032318EQS066O.

Iervolino I., Cito P., Felicetta C., Lanzano G. and Vitale A.; 2021: *Exceedance of design actions in epicentral areas: insights from the ShakeMap envelopes for the 2016–2017 Central Italy sequence.* Bull. Earthq. Eng., 19, 5391–5414, doi: 10.1007/s10518-021-01192-z.

Iervolino I., Cito P., De Falco M., Festa G., Hermann M., Lomax A., Marzocchi W., Santo A., Strumia C., Massaro L., Scala A., Scotto di Uccio F. and Zollo A.; 2024: *Seismic risk mitigation at Campi Flegrei in volcanic unrest.* Nat. Commun., 15, 10474, doi: 10.1038/s41467-024-55023-1.

Lowes L., Mitra N. and Altoontash A.; 2004: *A beam-column joint model for simulating the earthquake response of reinforced concrete frames.* PEER Report 2003/10, Pacific Earthquake Engineering Research Center, Berkeley, CA, USA, 59 pp.

Manfredi G.; 2001: *Evaluation of seismic energy demand.* Earthq. Eng. Struct. Dyn., 30, 485–499, doi: 10.1002/eqe.17.

Michelini A., Faenza L., Lanzano G., Lauciani V., Jozinović D., Puglia R. and Luzi L.; 2019: *The new ShakeMap in Italy: progress and advances in the last 10 yr.* Seismol. Res. Lett., 91, 317–333, doi: 10.1785/0220190130.

Ramadan F., Smerzini C., Lanzano G. and Pacor F.; 2021: *An empirical model for the vertical-to-horizontal spectral ratios for Italy.* Earthq. Eng. Struct. Dyn., 50, 4121–4141, doi: 10.1002/eqe.3548.

RINTC-Workgroup; 2018: *Results of the 2015–2017 Implicit Seismic Risk of Code-Conforming Structures in Italy (RINTC) Project.* ReLUIS Report, Rete dei Laboratori Universitari di Ingegneria Sismica (ReLUIS), Naples, Italy.

Scotto di Uccio F., Lomax A., Natale J., Muzellec T., Festa G., Nazeri S., Convertito V., Bobbio A., Strumia C. and Zollo A.; 2024: *Delineation and fine-scale structure of fault zones activated during the 2014–2024 unrest at the Campi Flegrei caldera (southern Italy) from high-precision earthquake locations.* Geophys. Res. Lett., 51, e2023GL107680, doi: 10.1029/2023GL107680.

Stucchi M., Meletti C., Montaldo V., Crowley H., Calvi G.M. and Boschi E.; 2011: *Seismic hazard assessment (2003–2009) for the Italian Building Code.* Bull. Seismol. Soc. Am., 101, 1885–1911, doi: 10.1785/0120100130.

Suzuki A. and Iervolino I.; 2017: *Italian vs worldwide history of largest PGA and PGV.* Ann. Geophys., 60, S055, doi: 10.4401/ag-7391.

Suzuki A. and Iervolino I.; 2021: *Seismic fragility of code-conforming Italian buildings based on SDoF approximation.* J. Earthq. Eng., 25, 2873–2907, doi: 10.1080/13632469.2019.1657989.

Tusa G. and Langer H.; 2016: *Prediction of ground motion parameters for the volcanic area of Mount Etna.* J. Seismol., 20, 1–42, doi: 10.1007/s10950-015-9508-x.

Wald D.J., Quitoriano V., Heaton T.H., Kanamori H., Scrivner C.W. and Worden C.B.; 1999: *TriNet "ShakeMaps": rapid generation of peak ground motion and intensity maps for earthquakes in southern California.* Earthq. Spectra, 15, 537–555, doi: 10.1193/1.1586057.

Worden C.B., Thompson E.M., Baker J.W., Bradley B.A., Luco N. and Wald D.J.; 2018: *Spatial and spectral interpolation of ground-motion intensity measure observations.* Bull. Seismol. Soc. Am., 108, 866–875, doi: 10.1785/0120170201.

*Corresponding author:* Pasquale Cito
Dipartimento di Strutture per l'Ingegneria e l'Architettura, Università degli Studi di Napoli Federico II
Via Claudio 21, Napoli, Italy
Phone: +39 081 7683488; e-mail: pasquale.cito@unina.it

## Appendix A

Table A1 shows, for each of the events considered in the earthquake engineering analysis discussed in the study, the date, epicentre coordinates, duration magnitude ($M_d$), hypocentral depth, number of recorded three-component records ($n$), minimum and maximum epicentral distance at which they were recorded ($R_{epi,min}$ and $R_{epi,max}$, respectively), and maximum recorded horizontal and vertical *PGA* ($PGA_{max,H}$ and $PGA_{max,V}$, respectively).

Table A 1 - Metadata for the earthquakes considered in the engineering analysis presented in the study.

| Date | Lat. N [°] | Long. E [°] | $M_d$ | Depth [km] | $n$ | $R_{epi,min}$ [km] | $R_{epi,max}$ [km] | $PGA_{max,H}$ [g] | $PGA_{max,V}$ [g] |
|---|---|---|---|---|---|---|---|---|---|
| 16/03/2022 14:14:34 | 40.8272 | 14.1402 | 3.5 | 3 | 24 | 0.9 | 97.7 | 0.132 | 0.064 |
| 29/03/2022 17:45:32 | 40.8313 | 14.1557 | 3.6 | 3 | 9 | 2.1 | 29.5 | 0.061 | 0.058 |
| 08/05/2023 2:28:34 | 40.83 | 14.138 | 3.4 | 3 | 17 | 0.7 | 86.5 | 0.123 | 0.063 |
| 08/05/2023 22:33:17 | 40.826 | 14.1365 | 2.8 | 2 | 7 | 0.6 | 7.7 | 0.040 | 0.027 |
| 18/08/2023 4:18:05 | 40.8315 | 14.1418 | 3.3 | 2 | 45 | 1.0 | 98.0 | 0.132 | 0.098 |
| 07/09/2023 17:45:28 | 40.83 | 14.147 | 3.8 | 3 | 52 | 1.4 | 97.1 | 0.094 | 0.097 |
| 27/09/2023 1:35:34 | 40.8172 | 14.156 | 4.2 | 3 | 59 | 0.9 | 97.5 | 0.087 | 0.086 |
| 02/10/2023 20:08:26 | 40.8302 | 14.1495 | 4 | 3 | 42 | 1.6 | 96.9 | 0.067 | 0.056 |
| 16/10/2023 10:36:21 | 40.8268 | 14.1423 | 3.6 | 2 | 11 | 1.1 | 61.6 | 0.064 | 0.061 |
| 21/01/2024 9:35:04 | 40.8075 | 14.1018 | 2.6 | 4 | 11 | 2.2 | 7.5 | 0.017 | 0.015 |

Table A 1 - continued.

| Date | Lat. N [°] | Long. E [°] | $M_d$ | Depth [km] | $n$ | $R_{epi,min}$ [km] | $R_{epi,max}$ [km] | $PGA_{max,H}$ [g] | $PGA_{max,V}$ [g] |
|---|---|---|---|---|---|---|---|---|---|
| 04/04/2024 5:14:36 | 40.8228 | 14.1138 | 2.9 | 3 | 15 | 0.6 | 5.9 | 0.072 | 0.057 |
| 04/04/2024 5:32:56 | 40.8228 | 14.1142 | 3.2 | 3 | 4 | 4.4 | 63.4 | 0.004 | 0.003 |
| 06/04/2024 11:59:31 | 40.7983 | 14.1127 | 2.5 | 3 | 16 | 2.6 | 18.7 | 0.015 | 0.009 |
| 14/04/2024 7:44:24 | 40.8282 | 14.1368 | 3.7 | 3 | 49 | 0.6 | 97.9 | 0.161 | 0.087 |
| 14/04/2024 8:01:43 | 40.8293 | 14.1383 | 2.8 | 2 | 19 | 0.7 | 61.3 | 0.065 | 0.051 |
| 16/04/2024 3:38:05 | 40.83 | 14.1498 | 2.5 | 3 | 15 | 0.9 | 8.9 | 0.028 | 0.026 |
| 27/04/2024 3:44:56 | 40.8113 | 14.0943 | 3.9 | 3 | 61 | 2.1 | 99.6 | 0.123 | 0.095 |
| 07/05/2024 1:47:54 | 40.827 | 14.1447 | 3.2 | 2 | 19 | 0.4 | 40.2 | 0.058 | 0.076 |
| 07/05/2024 17:37:25 | 40.8253 | 14.1378 | 2.7 | 2 | 16 | 0.5 | 7.8 | 0.095 | 0.047 |
| 08/05/2024 5:29:10 | 40.836 | 14.1247 | 2.6 | 3 | 15 | 0.7 | 7.5 | 0.050 | 0.025 |
| 10/05/2024 11:25:51 | 40.8047 | 14.1055 | 3.7 | 3 | 31 | 2.2 | 89.2 | 0.064 | 0.026 |
| 13/05/2024 1:30:20 | 40.8283 | 14.0873 | 2.9 | 4 | 21 | 0.5 | 60.7 | 0.059 | 0.064 |
| 18/05/2024 4:30:55 | 40.835 | 14.1467 | 2.8 | 3 | 16 | 1.3 | 8.9 | 0.078 | 0.057 |
| 20/05/2024 17:51:14 | 40.8358 | 14.1305 | 3.5 | 3 | 33 | 0.8 | 85.6 | 0.214 | 0.110 |
| 20/05/2024 18:10:03 | 40.8277 | 14.138 | 4.4 | 3 | 68 | 0.6 | 98.0 | 0.366 | 0.207 |
| 20/05/2024 19:46:14 | 40.8263 | 14.138 | 3.9 | 3 | 33 | 2.7 | 98.2 | 0.025 | 0.016 |
| 20/05/2024 19:55:37 | 40.824 | 14.1287 | 3.1 | 3 | 20 | 0.5 | 61.9 | 0.123 | 0.077 |
| 20/05/2024 21:00:55 | 40.8228 | 14.1232 | 3.6 | 3 | 30 | 0.3 | 87.9 | 0.136 | 0.108 |
| 20/05/2024 22:55:54 | 40.8203 | 14.1435 | 2.8 | 0 | 16 | 0.4 | 12.8 | 0.018 | 0.018 |
| 22/05/2024 6:28:00 | 40.808 | 14.11 | 3.6 | 2 | 31 | 1.7 | 89.6 | 0.102 | 0.069 |
| 25/05/2024 1:03:23 | 40.8295 | 14.1402 | 3.7 | 2 | 18 | 0.7 | 29.2 | 0.051 | 0.032 |
| 08/06/2024 1:52:04 | 40.8282 | 14.1447 | 3.5 | 2 | 21 | 0.5 | 73.0 | 0.027 | 0.014 |
| 08/06/2024 2:09:03 | 40.8313 | 14.1517 | 3.7 | 3 | 35 | 1.1 | 86.9 | 0.111 | 0.089 |
| 08/06/2024 2:10:16 | 40.8282 | 14.146 | 2.7 | 2 | 1 | 1.6 | 1.6 | 0.016 | 0.007 |
| 18/06/2024 1:58:24 | 40.8283 | 14.0882 | 3.4 | 3 | 20 | 0.5 | 90.4 | 0.040 | 0.042 |

Table A 1 - continued.

| Date | Lat. N [°] | Long. E [°] | $M_d$ | Depth [km] | $n$ | $R_{epi,min}$ [km] | $R_{epi,max}$ [km] | $PGA_{max,H}$ [g] | $PGA_{max,V}$ [g] |
|---|---|---|---|---|---|---|---|---|---|
| 02/07/2024 13:13:45 | 40.8167 | 14.155 | 2.8 | 3 | 15 | 0.6 | 8.8 | 0.055 | 0.030 |
| 03/07/2024 0:18:44 | 40.8203 | 14.1577 | 3.2 | 3 | 26 | 0.3 | 87.4 | 0.068 | 0.036 |
| 11/07/2024 9:59:20 | 40.8352 | 14.1448 | 2.6 | 3 | 15 | 1.3 | 8.8 | 0.089 | 0.044 |
| 18/07/2024 6:08:37 | 40.8297 | 14.1468 | 3.6 | 2.4 | 93 | 0.2 | 110.2 | 0.173 | 0.146 |
| 26/07/2024 11:46:21 | 40.8075 | 14.098 | 4 | 4 | 51 | 2.1 | 99.5 | 0.113 | 0.054 |
| 18/08/2024 0:29:21 | 40.8183 | 14.1408 | 2.8 | 0 | 16 | 0.7 | 7.7 | 0.015 | 0.012 |
| 30/08/2024 19:23:15 | 40.8313 | 14.1478 | 3.7 | 2 | 36 | 0.9 | 87.0 | 0.086 | 0.097 |
| 13/10/2024 6:07:53 | 40.8345 | 14.1478 | 2.6 | 2 | 15 | 1.6 | 28.9 | 0.037 | 0.030 |
| 06/12/2024 4:33:59 | 40.8225 | 14.1353 | 3.4 | 1 | 27 | 0.6 | 64.2 | 0.029 | 0.018 |
| 06/12/2024 8:58:13 | 40.8192 | 14.1408 | 2.5 | 0 | 24 | 0.1 | 7.7 | 0.492 | 0.572 |
| 17/01/2025 16:53:50 | 40.829 | 14.1328 | 3 | 2 | 29 | 0.2 | 82.4 | 0.187 | 0.107 |
| 05/02/2025 10:00:32 | 40.8285 | 14.1488 | 2.7 | 3 | 24 | 0.1 | 8.7 | 0.079 | 0.053 |
| 13/02/2025 15:34:22 | 40.8307 | 14.1488 | 2.5 | 2 | 24 | 0.2 | 8.9 | 0.077 | 0.085 |
| 13/02/2025 22:18:28 | 40.8313 | 14.1462 | 2.6 | 2 | 24 | 0.3 | 8.7 | 0.056 | 0.036 |
| 16/02/2025 14:30:02 | 40.8097 | 14.1057 | 3.9 | 3 | 68 | 1.7 | 99.3 | 0.121 | 0.056 |
| 16/02/2025 22:45:12 | 40.8325 | 14.1477 | 3 | 2 | 27 | 0.4 | 39.6 | 0.084 | 0.054 |
| 16/02/2025 23:19:52 | 40.8288 | 14.1483 | 3.9 | 2 | 64 | 0.1 | 98.5 | 0.530 | 0.344 |
| 17/02/2025 7:12:10 | 40.8302 | 14.1423 | 3 | 3 | 28 | 0.4 | 75.2 | 0.136 | 0.075 |
| 17/02/2025 7:14:11 | 40.8243 | 14.138 | 2.8 | 2 | 24 | 0.5 | 7.7 | 0.060 | 0.041 |
| 17/02/2025 16:53:24 | 40.8278 | 14.1435 | 2.7 | 2 | 25 | 0.2 | 29.5 | 0.100 | 0.059 |
| 17/02/2025 17:15:54 | 40.8297 | 14.1475 | 2.6 | 3 | 23 | 0.5 | 8.7 | 0.063 | 0.045 |
| 09/03/2025 23:59:14 | 40.8303 | 14.0833 | 2.6 | 4 | 23 | 0.2 | 8.8 | 0.072 | 0.021 |
| 11/03/2025 2:04:09 | 40.827 | 14.1382 | 3 | 2 | 37 | 0.5 | 86.6 | 0.269 | 0.112 |
| 13/03/2025 0:25:02 | 40.8175 | 14.149 | 4.6 | 3 | 76 | 0.4 | 99.5 | 1.142 | 0.577 |
| 14/03/2025 18:44:10 | 40.8197 | 14.1575 | 3.5 | 3 | 45 | 0.9 | 97.2 | 0.175 | 0.189 |

Table A 1 - continued.

| Date | Lat. N [°] | Long. E [°] | $M_d$ | Depth [km] | $n$ | $R_{epi,min}$ [km] | $R_{epi,max}$ [km] | $PGA_{max,H}$ [g] | $PGA_{max,V}$ [g] |
|---|---|---|---|---|---|---|---|---|---|
| 15/03/2025 12:32:27 | 40.8297 | 14.1323 | 3.9 | 3 | 70 | 0.2 | 98.0 | 0.237 | 0.127 |
| 12/04/2025 21:29:15 | 40.8253 | 14.1355 | 2.9 | 2 | 24 | 0.6 | 7.6 | 0.037 | 0.035 |
| 13/05/2025 10:07:44 | 40.8245 | 14.1117 | 4.4 | 2.6 | 177 | 0.7 | 221.2 | 0.392 | 0.225 |
| 13/05/2025 10:22:43 | 40.8252 | 14.1218 | 3.5 | 3 | 57 | 0.5 | 97.3 | 0.185 | 0.075 |
| 13/05/2025 12:58:42 | 40.8358 | 14.1262 | 3.3 | 2.6 | 94 | 0.8 | 109.4 | 0.189 | 0.118 |
| 13/05/2025 13:01:07 | 40.8248 | 14.1248 | 2.7 | 3 | 24 | 0.5 | 6.8 | 0.044 | 0.029 |
| 14/05/2025 12:23:00 | 40.8383 | 14.1435 | 3.1 | 2.5 | 99 | 0.4 | 109.3 | 0.187 | 0.089 |
| 23/05/2025 10:44:16 | 40.8335 | 14.0855 | 2.6 | 3 | 22 | 0.2 | 8.8 | 0.029 | 0.033 |
| 05/06/2025 4:48:25 | 40.8297 | 14.1493 | 3.2 | 3 | 39 | 0.0 | 41.7 | 0.177 | 0.120 |
| 06/06/2025 17:31:06 | 40.828 | 14.135 | 3.2 | 2 | 93 | 0.4 | 110.0 | 0.197 | 0.110 |
| 07/06/2025 19:45:34 | 40.8188 | 14.1398 | 2.5 | 0 | 24 | 0.2 | 7.6 | 0.046 | 0.029 |
| 21/06/2025 3:00:12 | 40.8348 | 14.1237 | 3.2 | 3 | 28 | 0.9 | 51.9 | 0.124 | 0.055 |
| 30/06/2025 10:47:11 | 40.808 | 14.0958 | 4.6 | 4 | 69 | 1.3 | 99.5 | 0.077 | 0.051 |
| 03/07/2025 7:00:08 | 40.8352 | 14.1502 | 2.6 | 2 | 24 | 0.6 | 85.7 | 0.156 | 0.055 |
| 18/07/2025 7:14:22 | 40.817 | 14.1557 | 4 | 3 | 63 | 0.5 | 97.5 | 0.405 | 0.407 |
| 28/08/2025 19:53:23 | 40.831 | 14.093 | 3 | 2 | 23 | 0.3 | 8.1 | 0.113 | 0.029 |
| 31/08/2025 14:10:13 | 40.8182 | 14.1415 | 3.3 | 1 | 23 | 0.3 | 13.1 | 0.518 | 0.721 |
| 31/08/2025 14:36:41 | 40.8187 | 14.149 | 3.3 | 2 | 24 | 0.4 | 86.2 | 0.302 | 0.253 |
| 31/08/2025 22:40:38 | 40.8203 | 14.1392 | 2.5 | 0 | 18 | 0.5 | 6.3 | 0.016 | 0.011 |
| 31/08/2025 23:29:36 | 40.8187 | 14.1413 | 2.8 | 0 | 22 | 0.3 | 7.7 | 0.055 | 0.035 |
| 01/09/2025 2:55:45 | 40.8275 | 14.123 | 4 | 0 | 41 | 0.6 | 94.3 | 0.559 | 0.677 |
| 01/09/2025 8:24:22 | 40.8302 | 14.1517 | 2.7 | 3 | 22 | 0.2 | 9.0 | 0.148 | 0.069 |
| 01/09/2025 15:22:01 | 40.829 | 14.147 | 3.3 | 2 | 55 | 0.2 | 110.2 | 0.149 | 0.091 |